Carbohydrate Polymers 106 (2014) 384–392

Contents lists available at ScienceDirect

Carbohydrate Polymers

journal homepage: www.elsevier.com/locate/carbpol

Structural investigation of a neutral extracellular glucan from *Lactobacillus reuteri* SK24.003

Ming Miao[a,*], Yajun Ma[a], Bo Jiang[a], Chao Huang[a], Xiaohui Li[a], Steve W. Cui[a,b], Tao Zhang[a]

[a] State Key Laboratory of Food Science & Technology, Jiangnan University, 1800 Lihu Avenue, Wuxi, Jiangsu 214122, PR China
[b] Food Research Program, Agriculture and Agri-Food Canada, 93 Stone Road West, Guelph, Ont., Canada N1G 5C9

ARTICLE INFO

Article history:
Received 4 July 2013
Received in revised form 4 December 2013
Accepted 13 January 2014
Available online 21 January 2014

Keywords:
Lactobacillus reuteri SK 24.003
α-Glucan
Structural analysis
Anticorrosive property

ABSTRACT

The structural features of a neutral extracellular glucan derived from *Lactobacillus reuteri* SK24.003 were investigated. Colonies of the strain SK24.003 exhibited a creamy and slimy morphological appearance on MRS solid medium and were identified as *L. reuteri* via 16S rDNA sequence analysis. The exopolysaccharide produced from sucrose was composed exclusively of glucose, and the weight-average molecular weight was 4.31×10^7 g/mol. The polysaccharide exhibited an α-(1→4) backbone with an α-(1→6) branch at every fourth residue, as deduced from both NMR and GC–MS data. The exopolysaccharide acted as a natural steel corrosion inhibitor. The results suggested that a novel α-glucan produced by *L. reuteri* SK24.00 could be broadly used in food and material field.

1. Introduction

Extracellular polysaccharides are an abundant and diverse class of natural biopolymers and display special thickening, gelling, stabilizing or emulsifying properties. These properties position them as critical participants in the development of new products ranging from foods, nutraceuticals and pharmaceuticals (Badel, Bernardi, & Michaud, 2011; Freitas, Alves, & Reis, 2011; Hassan, 2007; Kumar, Mody, & Jha, 2007; Prajapati, Jani, Zala, & Khutliwala, 2013). Many microorganisms can synthesize extracellular polysaccharides that perform a wide variety of biological functions. These polymers may be assembled as capsular polysaccharides that are tightly associated with the cell surface or as slime polysaccharides that may be liberated into the growth medium (Hassan, 2007; Freitas et al., 2011). Bacterial exopolysaccharides can be composed of one type of sugar monomer (homopolysaccharides) or consist of several types of monomers (heteropolysaccharides) (Kumar et al., 2007).

Lactic acid bacteria are well known for their wide applications in the food, pharmaceutical and chemical industries. Particularly, lactic acid bacteria are generally regarded as safe (GRAS) and are extremely important in the industrial production of fermented foods, including dairy products, meat products and sourdoughs. Over the last decades, several strains of various genera within the lactic acid bacteria group have been demonstrated to synthesize extracellular polysaccharides (De Vuyst, De Vin, Vaningelgem & Degeest, 2001). These exopolysaccharides positively affect the texture, mouth-feel, taste perception and stability of yogurt, cheese or milk-based desserts (Badel et al., 2011; Hassan, 2007). Simultaneously, the prebiotic, anti-inflammatory, immunomodulatory, antitumor and antioxidant characteristics of exopolysaccharides have been investigated (Ai et al., 2008; Pan & Mei, 2010; Sreekumar & Hosono, 1998; Vinderola, Perdigón, Duarte, Farnworth, & Matar, 2006). Moreover, exopolysaccharides comprise a class of renewable polymers that display interesting anti-corrosive properties when applied to steel and represent sustainable alternatives to inorganic anti-corrosive pigments such as zinc phosphates (Finkenstadt, Côté, & Willett, 2011; Scheerder et al., 2012). The exopolysaccharides might adhere to immersed surfaces to form an organic film, which led to important interactions resulting in passivation and protection of the metal. Penninga et al., 2002 found an α-(1→3), α-(1→6)-linked D-glucan produced by *Lactobacillus reuteri* strain 180 that inhibited corrosion while dispersed in a electrolyte solution rather than as a coating. Purified *Leuconostoc mesenteroides* exopolysaccharide-B 1498L [α-(1→6) linked D-glucose units with α-(1→3) branching] coatings inhibited the corrosion of low-carbon steel without any flash corrosion (Finkenstadt et al., 2011). Roux, Bur, Ferrari, Tribollet, and Feugeas (2010) developed a new eco-friendly and corrosion-inhibiting admixture based on natural α-(1→3,1→6)-D-glucan exopolysaccharide from *L. reuteri* 180, using as a promising anti-corrosives for the corrosion inhibition

* Corresponding author at: State Key Laboratory of Food Science & Technology, 1800 Lihu Avenue, Wuxi, Jiangsu 214122, PR China. Tel.: +86 0510 853 27859; fax: +86 0510 859 19161.
E-mail address: miaoming@jiangnan.edu.cn (M. Miao).

0144-8617/$ – see front matter.
http://dx.doi.org/10.1016/j.carbpol.2014.01.047

on steel in seawater. They found that the corrosion inhibition induced by exopolysaccharide 180 admixture was more due to the modification of the cement-rebars interface than to the clogging of the cement porous network. Scheerder et al. (2012) reported that the exopolysaccharide 180 combined with a waterborne styrene-acrylic polymer dispersion gave an improvement in the anti-corrosive performance. The carboxylic acid groups on the oxidized exopolysaccharide formed a complex with iron ions formed by the anodic reaction and this insoluble complex formed a protective layer between the coating and metal. Moreover, the main extracellular polysaccharides from *Streptococcus thermophilus*, *Lactococcus lactis* and *Lactobacillus* spp. are heteropolysaccharides with repeating unites (Badel et al., 2011; De Vuyst et al., 2001). The objectives of the present work were to investigate the isolation, purification and characterization of an extracellular homopolysaccharide (HoEPS) derived from *L. reuteri* SK24.003 (LRHP) isolated from a traditional Chinese fermented dairy product. Elucidating the structural properties of HoEPS will allow its potential exploitation in industrial applications.

2. Materials and methods

2.1. Materials

$NaBD_4$ (isotopic purity 98 atom% D, Cat. No. 205591), anhydrous NaOH (purity ≥98%, Cat. No. S5861), anhydrous dimethylsulfoxide (purity ≥99.9%, Cat. No. 276855), deuterium oxide (isotopic purity 99.99 atom% D, Cat. No. 191701) and amylopectin from maize (Cat. No. 10120) were obtained from Sigma–Aldrich Co. (St. Louis, MO). dNTP mix, *Taq* DNA polymerase and *Taq* reaction buffer for PCR were purchased from Promega Co. (Shanghai, China). Methyl iodide (analytical grade) was from Tj Shield Co. (Tianjin, China). All other chemicals were of reagent grade and were obtained from Sinopharm Chemical Reagent Co., Ltd. (Shanghai, China).

2.2. Strains for exopolysaccharide production and growth media

The strain SK24.003 was isolated from a traditional Chinese fermented dairy product and cultivated in MRS medium containing 100 g/L sucrose, 10 g/L yeast extract, 1 mL/L tween 80, 20 g/L K_2HPO_4, 0.02 g/L $CaCl_2$, 0.2 g/L $MgSO_4{\cdot}7H_2O$, 0.01 g/L NaCl, 0.01 g/L $MnSO_4{\cdot}H_2O$, 0.01 g/L $FeSO_4{\cdot}7H_2O$, pH 6.8–7.0 at 37 °C for 24–48 h.

2.3. Identification of strain SK24.003

Morphological tests were used to characterize strain SK 24.003. The strain was propagated in traditional MRS medium containing 20 g/L agar at 37 °C for 48 h. The colony morphology was recorded using a digital camera (Canon, Shanghai, China). Strain identity was further confirmed by partial sequencing of the 16S rDNA gene. Bacterial universal primers of 27F (5′-CAGAGTTTGATCCTGGCT-3′) and 1540R (5′-AGGAGGTGATCCAGCCGCA-3′) were used to amplify bacterial 16S rRNA genes of target isolate. Polymerase chain reaction (PCR) mixture (25 μL) contained about 1 μL DNA template, 0.5 μL dNTP mix, 0.2 μL *Taq* DNA polymerase, 0.5 μL of each primer and 2.5 μL 10× *Tap* buffer. The PCR reaction was involved an initial denaturation at 94 °C for 5 min, 35 cycles of 94 °C for 30 s, 55 °C for 35 s and 72 °C for 1 min and extention for 8 min. The products were purified with the Qiagen PCR purification kit and sequenced by Sangon Biotech Company (Shanghai, China). The 16S rDNA sequence was aligned in GenBank of NCBI by using BLAST and analyzed with ClustalX 1.83 and MEGA 5.0 programs.

2.4. Isolation and purification of exopolysaccharides

The strain SK24.003 was inoculated into 500 mL of optimized fermentation medium and grown at 37 °C for 48 h in an anaerobic incubator. The culture was heated in a boiling water bath for 30 min, and then centrifuged at 10,000 × *g* for 20 min to separate the cells. Trichloroacetic acid (TCA) was added slowly to the cell-free supernatant under constant stirring to bring the TCA concentration to 4% (v/v). After centrifugation and ultrafiltration, the exopolysaccharide in the concentrated solution was precipitated by adding three volumes of 95% ethanol at room temperature. This solution was stored overnight at 4 °C. The sample was then centrifuged under the above conditions, and the precipitate was collected. The resulting sample was dissolved in deionized water and then dialyzed at 4 °C to remove the small sugars. The solution was freeze-dried and crude polysaccharide was obtained.

The crude polysaccharide (20 mg/mL) was loaded onto a DEAE-Sepharose Fast Flow column (2.6 cm × 30.0 cm, GE Healthcare, Fairfield, CT), eluted with two column volumes of deionized water and then eluted with a linear gradient of sodium chloride (0–1.0 M) at 4 °C. The eluted solution was collected at a flow rate of 1 mL/min. The fractions (6 min each) with the largest polysaccharide amount were further separated using gel filtration chromatography (GPC) on a Sepharose CL-2B column (1.6 cm × 50.0 cm, GE Healthcare, Fairfield, CT) equilibrated at 4 °C. Fractions (6 mL) were collected at a flow rate of 0.5 mL/min using deionized water as the mobile phase. The purified polysaccharide was lyophilized and stored in a vacuum desiccator prior to structural investigation.

2.5. Monosaccharide composition analysis

The monosaccharide composition was determined using high-performance anion-exchange chromatography coupled with pulsed amperometric detection (HPAEC-PAD). The polysaccharide (4 mg) was hydrolyzed with 2 M H_2SO_4 (2 mL) at 105 °C for 8 h to completely release the monosaccharide. After neutralization with $BaCO_3$ and centrifugation at 10,000 × *g* for 10 min, the supernatants were analyzed using an ICS-5000 HPAEC-PAD (Dionex, Sunnyvale, CA) equipped with an electrochemical detector with a gold working electrode and Ag/AgCl as a reference electrode. A CarboPac PA20 column (3 mm × 150 mm, Dionex, Sunnyvale, CA) connected to a CarboPac PA-1 guard column (4 mm × 50 mm, Dionex, Sunnyvale, CA) was used. Gradient elution system was used with a mixture eluent: 250 mM NaOH solution (A), 1 M sodium acetate solution (B) and ultrapure water. The initial mobile phase was only 1.8% A for 21 min. A gradient from 5% to 20% B was performed in next 9 min and 1.8% A was maintained in the period. Finally, just 80% A was used as mobile phase from 30 min to 50 min. The elution was carried out at a flow rate of 0.5 mL/min at 30 °C. A set of monosaccharides were used as standard samples, including glucose, fructose, galactose, L-sorbose, mannose and L-rhamnose.

2.6. Molecular weight analysis

The polysaccharide (0.5 mg/mL) was filtered through a 0.45 μm cellulose acetate filter (Whatman, Maidstone, UK) and injected into a high-performance size-exclusion chromatography (HPSEC) system with a DAWN HELEOS-II multi-angle laser-light scattering detector (MALLS) and an Optilab T-rEX refractive-index detector (RI) (Wyatt Technology, Santa Barbara, CA). The MALLS was equipped with a He–Ne laser working at 658.0 nm. A Shodex OHpak SB-808 HQ column (8 mm × 300 mm, Showa Denko K.K., Tokyo, Japan) with an OHpak SB-G guard column was used at 25 °C. The mobile phase was 0.1 M $NaNO_3$ solution containing 0.02% sodium azide at 0.5 mL/min flow rate. A value of 0.1460 was used as *dn*/*dc* for molar weight calculation, and data processing were performed

Fig. 1. Colonial morphology of strain SK 24.003 from Chinese traditional fermented dairy product.

with Wyatt Astra software (Version 5.3.4.14, Wyatt Technology, USA). Weight-average molecular weight (M_w), polydispersity index (M_w/M_n) and *z*-root mean square radius of gyration (R_z) were obtained using the second-order Berry method.

2.7. FT-IR analysis

The FT-IR spectrum of the polysaccharide was recorded on a Nicolet Nexus 470 FT-IR spectrometer (Thermo Electron Co., Waltham, MA) at room temperature. The polysaccharide powder was blended with KBr at a 1:100 ratio and pressed into tablets before measurement. The spectrum was recorded at the absorbance mode from 400 to 4000 cm^{-1} at a resolution of 4 cm^{-1} with 32 scans using Omnic software (version 7.0).

2.8. Methylation analysis

The polysaccharide sample (20 mg) was methylated twice according to Cui (2005). Complete methylation was confirmed through the disappearance of the OH bond (3200–3700 cm^{-1}) in the FT-IR spectrum. The methylated product was recovered by dialysis and freeze-dried; it was then hydrolyzed with 4 M trifluoroacetic acid at 100 °C for 6 h, reduced with $NaBD_4$ (25 mg) under alkaline conditions and acetylated with acetic anhydride at 100 °C for 2 h to produce partially methylated alditol acetates (PMAA). The PMAA were analyzed using a gas chromatography–mass spectrometry (GC–MS) system equipped with a trace mass spectrometer and a DB-5 capillary column (0.25 mm × 30 m × 0.25 μm, Thermo Finnigan Co., Santa Clara, CA). Temperature program consisted of a ramp from 160 °C to 210 °C (8 min hold) at a rate of 3 °C/min, increased to 250 °C (6 min hold) at 8 °C/min using helium as the carrier gas at the flow rate of 1.0 mL/min. Identification of the sugar components and linkages was based on matching the PMAA mass spectra from the Complex Carbohydrate Research Center Spectral Database-PMAA (http://www.ccrc.uga.edu/specdb/ms/pmaa/pframe.html).

2.9. NMR analysis

The ^1H and ^{13}C spectra were recorded at 70 °C using a 400 MHz AVANCE III NMR spectrometer (Bruker Co., Billerica, MA). The polysaccharide sample (60 mg) was exchanged with deuterium in three rounds of lyophilization with 99.99% deuterium oxide and then dissolved in 0.45 mL 99.99% deuterium oxide. Using MestReNova software (version 8.0), chemical shifts (δ) were expressed in ppm and referenced internally with acetone and 1, 4-dioxan for ^1H and ^{13}C NMR spectra, respectively.

2.10. Anticorrosion effect

The polysaccharide sample was dissolved in 6.0% (w/v) calcium chloride or magnesium chloride aqueous solutions at a concentration of 0.5% (w/v). The solution was stirred for 10 min until the polysaccharide was completely dissolved and then was transferred to a glass tube. A no. 1 size steel metal paper clip was added and kept in the open system at 30 °C for 7 days. A control tube was prepared using salt solution without the polysaccharide.

3. Results and discussion

3.1. Identification of the SK24.003 strain

The SK24.003 strain was isolated from a traditional Chinese fermented dairy product and selected for the present study. SK 24.003 (Fig. 1) exhibited a creamy and slimy colony morphology on MRS solid medium. According to Leathers and Côté (2008), mutagenized survivor colonies were initially screened for a typical colony morphology that might suggest changes in glucan production. Thus, SK24.003 displayed a mucoid phenotype that indicated the presence of soluble exopolysaccharides. The 16S rDNA sequence (1465 base pairs, PCR amplified) of the strain SK24.003 was determined (Fig. 2A) and has been deposited in GenBank under the accession number JX963641. The nucleotide sequences were used for the analysis of similarity in the NCBI database using BLAST program. A phylogenetic tree was constructed (Fig. 2B) using ClustalX 1.83 and MEGA 5.0 software (Arizona State University, Tempe, AZ, USA). Strain SK24.003 was 96% similar to *L. reuteri* L7 and was thus identified as and named *L. reuteri* SK24.003. The strain was deposited in the China Center for Type Culture Collection (CCTCC) under accession number M 2011397.

3.2. Preparation and purification

To evaluate the structure of HoEPS from *L. reuteri* SK24.003, static fermentation was performed in flasks of medium containing sucrose at an initial concentration of 100 g/L. After 48 h of fermentation, HoEPS reached a concentration of 37.85 g/L. Crude water-soluble exopolysaccharides were obtained from the *L. reuteri* SK24.003 culture supernatant and purified using a DEAE-Sepharose Fast Flow column. The recovery of the eluted polysaccharides was about 84.72%. The crude polysaccharide yield for F1 (neutral polysaccharide) and F2 (acidic polysaccharide) were 57.55% and 27.17%, respectively (Fig. 3A). F1 was the dominant fraction and was applied to a Sepharose CL-2B column and eluted with deionized water. The elution profile (Fig. 3B) showed that F1 was a homogeneous polysaccharide and formed a single peak. The neutral polysaccharide in F1 was used in subsequent analyses.

A

```
1    TGCAAGTCGT ACGCACTGGC CCAACTGATT GATGGTGCTT GCACCTGATT GACGATGGAT
61   TACCAGTGAG TGGCGGACGG GTGAGTAACA CGTAGGTAAC CTGCCCCGGA GCGGGGGATA
121  ACATTTGGAA ACAGATGCTA ATACCGCATA ACAACAAAAG CCACATGGCT TTTGTTTGAA
181  AGATGGCTTT GGCTATCACT CTGGGATGGA CCTGCGGTGC ATTAGCTAGT TGGTAAGGTA
241  ACGGCTTACC AAGGCGATGA TGCATAGCCG AGTTGAGAGA CTGATCGGCC ACAATGGAAC
301  TGAGACACGG TCCATACTCC TACGGGAGGC AGCAGTAGGG AATCTTCCAC AATGGGCGCA
361  AGCCTGATGG AGCAACACCG CGTGAGTGAA GAAGGGTTTC GGCTCGTAAA GCTCTGTTGT
421  TGGAGAAGAA CGTGCGTGAG AGTAACTGTT CACGCAGTGA CGGTATCCAA CCAGAAAGTC
481  ACGGCTAACT ACGTGCCAGC AGCCGCGGTA ATACGTAGGT GGCAAGCGTT ATCCGGATTT
541  ATTGGGCGTA AAGCGAGCGC AGGCGGTTGC TTAGGTCTGA TGTGAAAGCC TTCGGCTTAA
601  CCGAAGAAGT GCATCGGAAA CCGGGCGACT TGAGTGCAGA AGAGGACAGT GGAACTCCAT
661  GTGTAGCGGT GGAATGCGTA GATATATGGA AGAACACCAG TGGCGAAGGC GGCTGTCTGG
721  TCTGCAACTG ACGCTGAGGC TCGAAAGCAT GGGTAGCGAA CAGGATTAGA TACCCTGGTA
781  GTCCATGCCG TAAACGATGA GTGCTAGGTG TTGGAGGGTT TCCGCCCTTC AGTGCCGGAG
841  CTAACGCATT AAGCACTCCG CCTGGGGAGT ACGACCGCAA GGTTGAAACT CAAAGGAATT
901  GACGGGGGCC CGCACAAGCG GTGGAGCATG TGGTTTAATT CGAAGCTACG CGAAGAACCT
961  TACCAGGTCT TGACATCTTG CGCTAACCTT AGAGATAAGG CGTTCCCTTC GGGGACGCAA
1021 TGACAGGTGG TGCATGGTCG TCGTCAGCTC GTGTCGTGAG ATGTTGGGTT AAGTCCCGCA
1081 ACGAGCGCAA CCCTTGTTAC TAGTTGCCAG CATTAAGTTG GGCACTCTAG TGAGACTGCC
1141 GGTGACAAAC CGGAGGAAGG TGGGGACGAC GTCAGATCAT CATGCCCCTT ATGACCTGGG
1201 CTACACACGT GCTACAATGG ACGGTACAAC GAGTCGCAAG CTCGCGAGAG TAAGCTAATC
1261 TCTTAAAGCC GTTCTCAGTT CGGACTGTAG GCTGCAACTC GCCTACACGA AGTCGGAATC
1321 GCTAGTAATC GCGGATCAGC ATGCCGCGGT GAATACGTTC CCGGGCCTTG TACACACCGC
1381 CCGTCACACC ATGGGAGTTT GTAACGCCCA AAGTCGGTGG CCTAACCTTT ATGGAGGGAG
1441 CCGCCTAAGG CGGGACAGAT GACTG
```

B

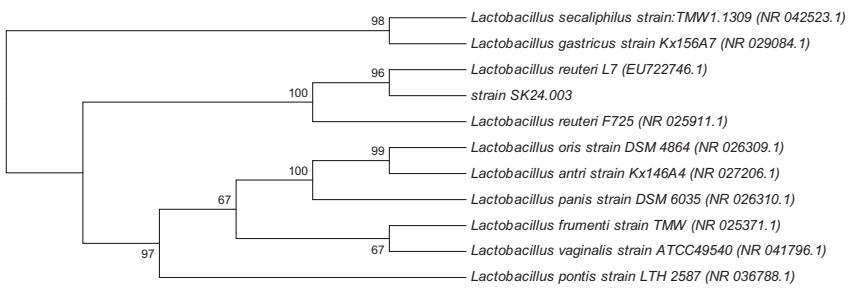

Fig. 2. Nucleotide sequences (A) and phylogenetic tree (B) of strain SK 24.003.

3.3. Composition analysis

The sugar composition of the F1 was analyzed using HPAEC-PAD. Only glucose was detected upon the total acid hydrolysis of F1, consistent with the proposed homogeneous composition of the lactobacillus exopolysaccharides suggested by Bounaix et al. (2009). Lactic acid bacteria, including the *Lactobacilli* and *L. mesenteroides* strains used in sourdough, produce a variety of homopolysaccharides containing either fructose or glucose. They are synthesized in larger amounts (g/L) from sucrose by secreted or cell anchored glucansucrases and fructansucrases that convert sucrose into fructans (levan or inulin) or glucans (dextran, alternan, reuteran or mutan) and concomitantly release either fructose or glucose, respectively.

3.4. Molecular weight analysis

The molecular weight of the HoEPS was measured using HPSEC-MALLS-RI, and the results are presented in Table 1. The weight-average molecular weight (M_w), polydispersity index (M_w/M_n, where M_n is the number-average molecular weight) and *z*-root mean square radius of gyration (R_z) of HoEPS were 4.31×10^7 g/mol, 1.17 and 43.6 nm, respectively. Bounaix et al. (2009) and Freitas et al. (2011) reported that the molecular weights of the homopolysaccharides from lactic acid bacteria ranged from 10^6 to 10^9 g/mol, consistent with our result. The exopolysaccharide molecular weight difference might be attributed to the strain, fermentation parameters or analysis method. Based on the report of Ai et al. (2008), the M_w/M_n value in the present study indicated a rather narrow M_w distribution, indicative of a homogeneous molecular size distribution in the F1 isolated from *L. reuteri* SK24.003.

3.5. FT-IR analysis

The FTIR spectroscopic investigation results in the mid-infrared region demonstrated that the HoEPS and amylopectin spectra were similar (Fig. 4). The bands visible at approximately 3400 cm^{-1}, 2930 cm^{-1} and 1000–1200 cm^{-1} are common to all polysaccharides and represent O—H stretching and C—H stretching of the —CH_2 groups and saccharides, respectively (Cakić, Mitić, Nikolić, Ilić & Nikolić, 2008; Cui, 2005; Miao et al., 2014; Shingel, 2002). The broader absorption band at 3426.34 cm^{-1} in the HoEPS spectrum can be attributed to the stretching vibration of the hydroxyl group, which is due to the valent vibration of OH groups and valent vibration of H_2O constitutional molecules, as suggested by Mitić,

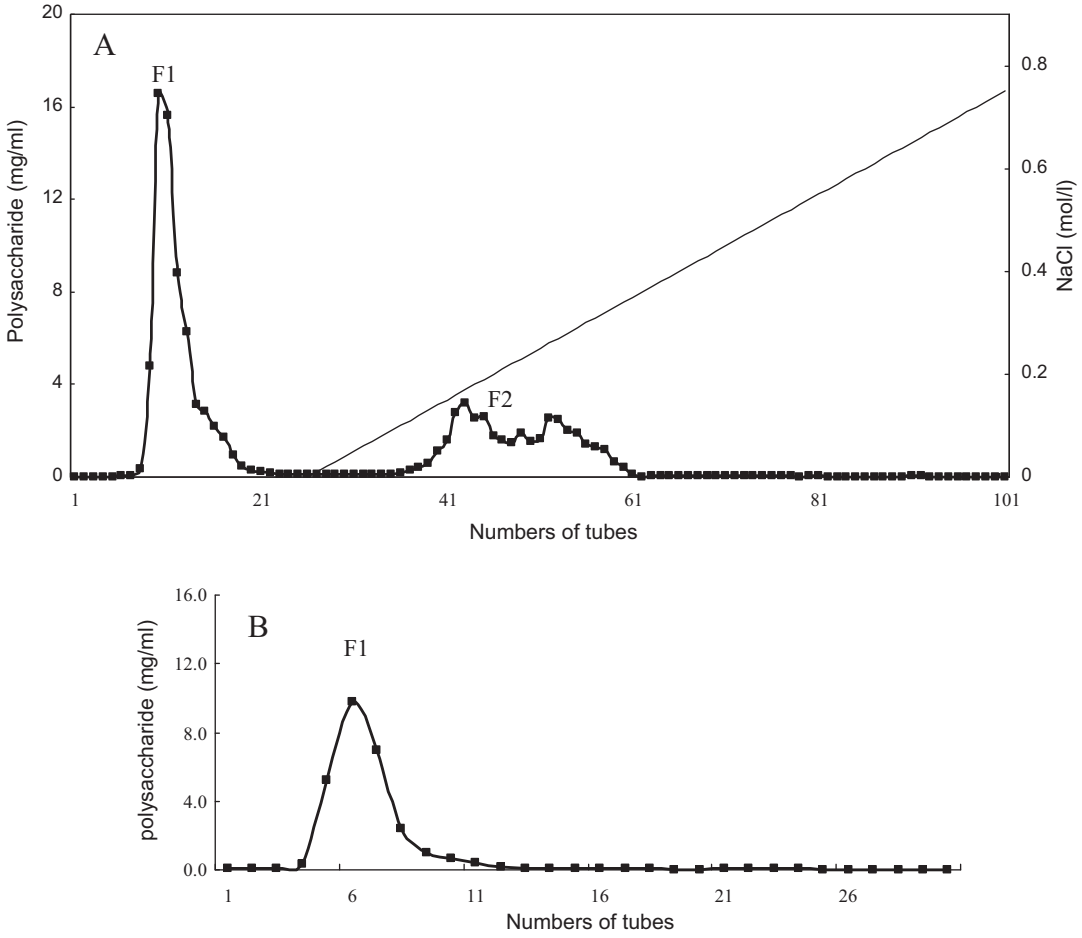

Fig. 3. Elution graphs of polysaccharide from strain SK 24.003 on DEAE Fast Flow column (A) and Speharose CL-2B column (B). F1 was loaded on the Sepharose CL-2B column.

Table 1
Molecular weight analysis, NMR analysis and methylation analysis of HoEPS from strain SK 24.003.

	HoEPS from SK24.003		Parameter
Molecular weight analysis	M_w (10^7 g/mol)		4.31 ± 0.36
	M_w/M_n		1.17 ± 0.53
	R_z (nm)		43.6 ± 3.6
NMR analysis	α-(1→4) (%)		79.6 ± 0.5
	α-(1→6) (%)		20.4 ± 1.6
Methylation analysis	1,5-Diacetyl-2,3,4,6-tetra-*O*-methyl glucitol	Glcp-(1→(%)	8.7 ± 1.1
	1,5,4-Triacetyl-2,3,6-tri-*O*-methyl glucitol	→4)-Glcp-(1→(%)	63.4 ± 1.7
	1,5,6-Triacetyl-2,3,4-tri-*O*-methyl glucitol	→6)-Glcp-(1→(%)	15.3 ± 1.4
	1,4,5,6-Tetraacetyl-2,3-di-*O*-methyl glucitol	→4, 6)-Glcp-(1→(%)	12.6 ± 0.8

Nikolić, Cakić, Premović, and Ilić (2009). The bands at 2926.95 cm^{-1} and 1632.25 cm^{-1} can be attributed to the C—H stretching vibration and associated water bending vibration, respectively (Mitić et al., 2011, 2009). The spectrum also exhibited a C—H deformation at 1410.30 cm^{-1} and 1373.31 cm^{-1}. In the 1000–1200 cm^{-1} region, three characteristic fingerprint peaks appeared at 1021.89, 1083.85 and 1157.53 cm^{-1}. The band at approximately 1157 cm^{-1} was attributed to the stretching vibrations of the C—O—C bond and the glycoside bridge (Cakić et al., 2008; Shingel, 2002). The broad peak at 1121 cm^{-1} most likely is due to the vibration of the C—O bond at the C4 position of the glucopyranose units (Mitić, Cakić & Nikolić, 2010; Mitić et al., 2009). Complex vibrations involving the stretching of the C6—O6 bond, along with deformational vibrations of the C4—C5 bond, result in the appearance of a band at 1083 cm^{-1} (Mitić et al., 2009). The bands in the region between 1000 cm^{-1} and 700 cm^{-1} (at approximately 929, 855, 762 and 708 cm^{-1}) were attributed to mixed CCH deformation vibrations coupled with CCO, OCO, and COC bending. Both the number and frequencies of the bands in the IR range depend on the conformation of the D-glucopyranose units. The glucopyranose units exist in six different typical conformations (1C, C1, 1B, B1, 3B, and B3) as reported by Cakić et al. (2008) and Mitić et al. (2009). The similarities to the γ(C—H) range indicate that there is no difference in the conformation of the glucopyranose unit in the HoEPS and amylopectin, and they most likely exhibit a C1 chair conformation (916 and 850 cm^{-1}). The peak near 929 cm^{-1} was assigned to the skeletal mode vibrations of α-(1→4) glycosidic linkages, and the peaks near 710, 600, 570, and 525 cm^{-1} corresponded to the ring deformations and scaffold vibrations (Santha, Sudha, Vijayakumari, Nayar & Moorthy, 1990; Mitić et al., 2009). According to Shingel (2002), the sharp peaks at approximately 1020 cm^{-1} in the spectra indicated the presence of the α-(1→6) linkage. The data suggested

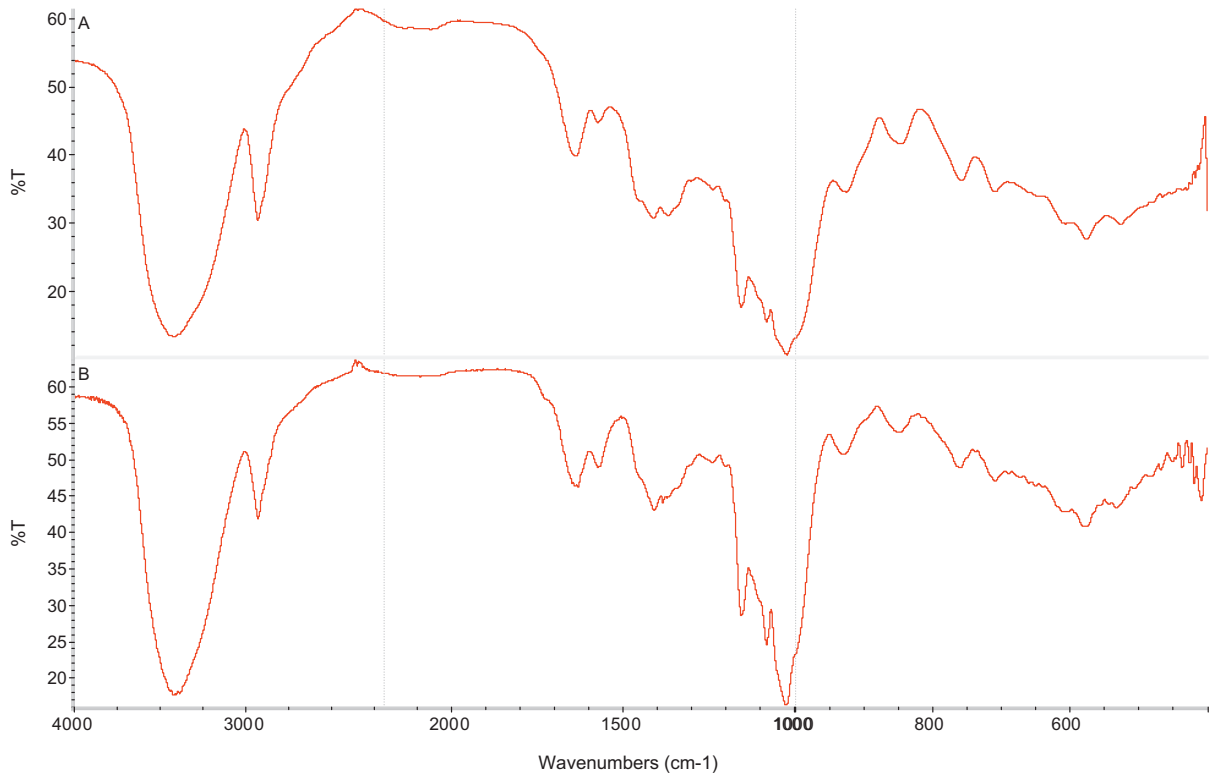

Fig. 4. FT-IR spectra of HoEPS from strain SK 24.003 (A) and amylopectin (B).

that HoEPS from *L. reuteri* SK24.003 exhibited an α-(1→4) backbone and an α-1,6 branched structure.

3.6. Methylation analysis

To determine the linkage pattern of HoEPS, F1 was subjected to methylation and GC–MS analysis. The identification and the proportions of methylated alditol acetates are listed in Table 1. The GC–MS results revealed the following four methylated alditol acetates with the relative contents of 8.7%, 63.4%, 15.3% and 12.6%, respectively. Moreover, the percentage of the non-reducing terminal (8.7%) was lower than the percentage of the branching residues of glucose (12.6%), which contradicted the general rule that every branch possesses one non-reducing terminal. This disagreement may be due firstly, to the different response at the detector of the terminal and branched derivatives and secondly, to the highly volatile character of the terminal residue that is easily lost during work up. The above results suggested that the exopolysaccharide F1 from *L. reuteri* SK24.003 was a highly branched soluble glucan that possessed predominantly α-(1→4) glycosidic linkages, with fewer α-(1→6) glycosidic linkages and α-(1→4,6) branching points. Kang, Kimura, and Kim (2011) reported that glucansucrase from lactobacilli synthesized a branched glucan with α-(1→4), α-(1→6), α-(1→4,6) glucosidic bonds, which might be extremely similar to the exopolysaccharide characterized here. This novel glucansucrase displayed a high hydrolysis/transferase activity ratio and produced a soluble glucan with a unique structure (reuteran) containing the highest amount of α-(1→4) glucosidic linkages as well as α-(1→6)-linked glucosyl units and 4,6-disubstituted α-glucosyl units at the branching points (Leemhuis et al., 2013).

3.7. NMR analysis

HoEPS was further analyzed using NMR spectroscopy, and the ^{1}H and ^{13}C spectra (Fig. 5) demonstrated an α-anomeric configuration for all glucose residues. In the anomeric region, two major signals appeared at δ 5.36 and 4.96 ppm; these were assigned to an anomeric proton of α-(1→4) linked D-glucopyranose and α-(1→6) linked D-glucopyranose units, respectively (Gidley, 1985; Kang et al., 2011; Maina, Tenkanen, Maaheimo, Juvonen, & Virkki, 2008; Miao et al., 2014). As illustrated in Fig. 5A, the α-(1→4) signal was split into two overlapping broad peaks, indicating that there were more than two significantly different structural elements in the α-D-glucopyranose-(1→4) residues (van Leeuwen, Leeflang, Gerwig, & Kamerling, 2008). The poor NMR spectral resolution precluded the trace of the terminal and α-(1→4, 6)-linked residues as indicated by the methylation analysis. In addition, the HoEPS was expressed as a ratio of α-(1→4) linkages to α-(1→6) linkages of approximately 4:1, which agreed with the overall substitution pattern observed by methylation analysis. According to the previous reports of Gidley (1985), the ratio of the α-(1→4) linkages to α-(1→6) linkages of amylopectin was 23, which was much higher than that of HoEPS, indicating that a structural difference might be biological in origin (Miao et al., 2014).

In the anomeric region (85–105 ppm) as shown in Fig. 5B, the major carbon resonances occurred at δ 100.12 ppm, which corresponded to C-1 of 4-linked glucose units. The anomeric region also harbored two minor peaks (99.01 and 98.46 ppm) associated with the branching and nonreducing-terminal sugars, as suggested by Seymour, Knapp and Bishop (1976). Four major signals in the nonanomeric region (60–85 ppm) at δ 72.06, 73.78, 70.60 and 71.78 ppm were attributed to the C-2, C-3, C-4 and C-5 substituted glucose residues, respectively, whereas the signal that appeared at δ 69.4 ppm corresponded to C-6 of the 4,6-linked units and those at 70.6 and 61.11 ppm were attributed to the C-4 and C-6 of nonreducing terminal residues, respectively, as suggested by Dais and Perlin (1982). The peak at δ 77.77 ppm was attributed to the signals of the downfield shift of the α-(1→4) linked D-glucopyranose units, similar to the dextran and pullulan produced by *L. mesenteroides* B-1254 (Seymour et al., 1976). The splitting of the anomeric

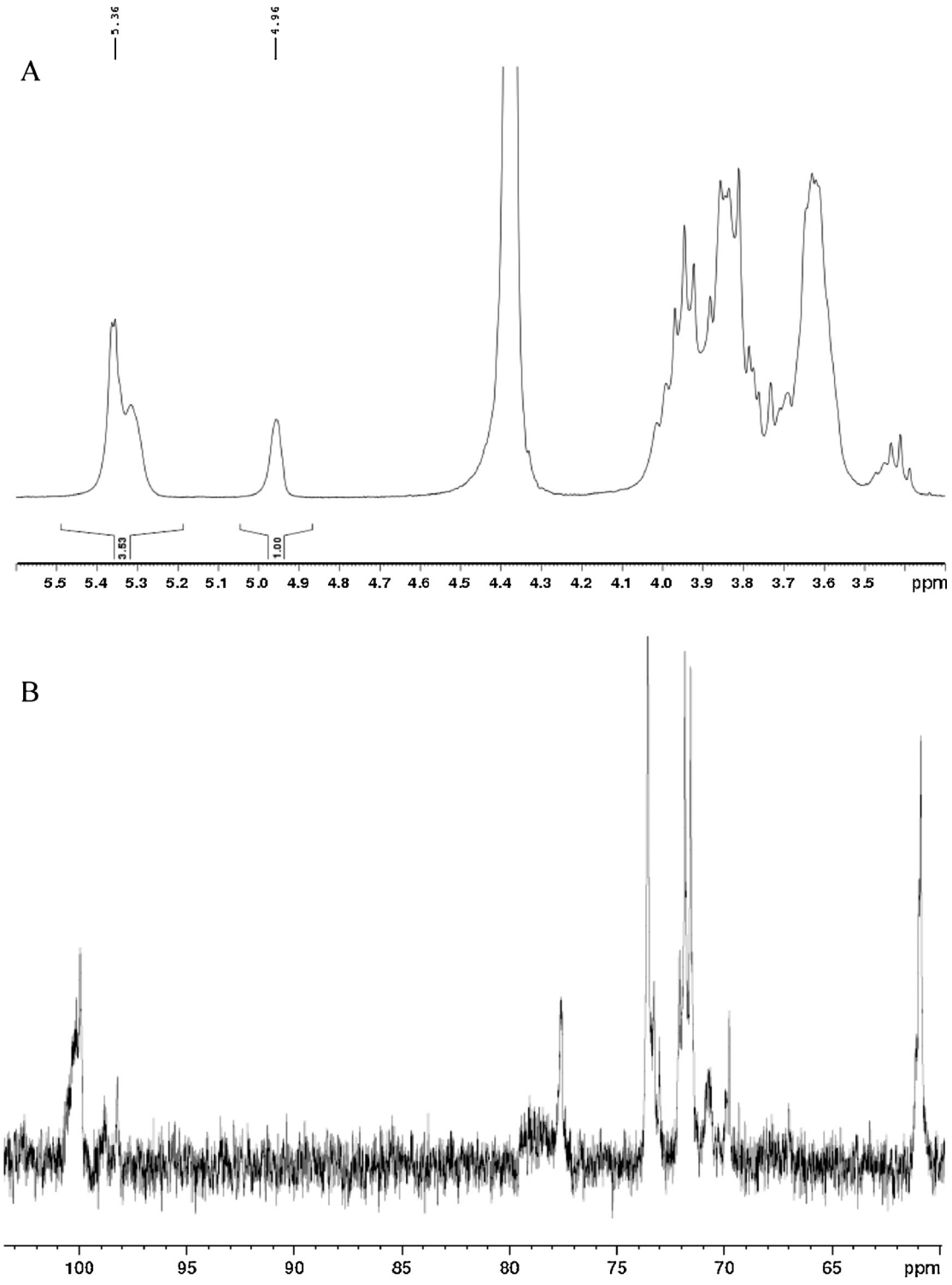

Fig. 5. ^{1}H (A) and ^{13}C (B) NMR spectra of HoEPS from SK24.003.

carbon (δ 100.12 ppm) and C-4 chemical-shift (δ 77.77 ppm) were also observed, which provided the basis for the structural explanation of repeating α-(1→4) and α-(1→6)-linked D-glucosyl residues. A minor peak near 70.00 ppm was due to branching and nonreducing end-group sugars. The ^{13}C spectrum was in complete agreement with the ^{1}H and FT-IR spectra, which indicated that the HoEPS was mainly composed of α-(1→4) and α-(1→6) linked D-glucopyranose units.

3.8. Anticorrosion analysis

The anticorrosion effects of HoEPS and amylopectin on the steel metal paper clip in the calcium chloride and magnesium chloride solutions are presented in Fig. 6. We observed that the paper clip was silver in color with a smooth and finished surface, and the solution was clear and transparent on the first day storage. After 7 days of storage at 30 °C, both the calcium chloride and magnesium

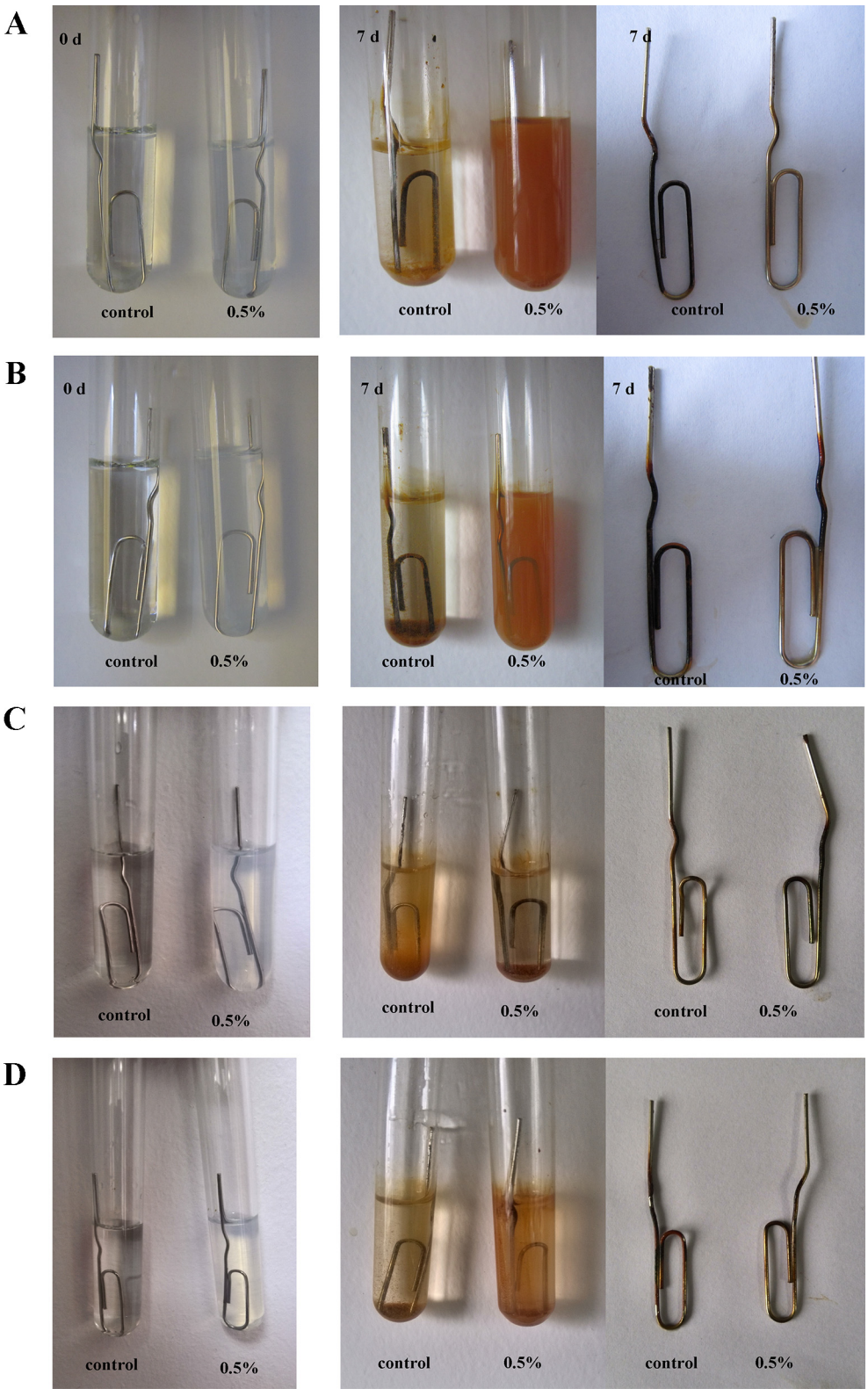

Fig. 6. Comparison of anticorrosion properties of HoEPS and amylopectin on steel metal paper clip at 30 °C for 7 days in salt solutions. (A) Calcium chloride solution with 0.5% HoEPS, (B) magnesium chloride solution with 0.5% HoEPS, (C) calcium chloride solution with 0.5% amylopectin, (D) magnesium chloride solution with 0.5% amylopectin.

chloride solutions were opaque, especially after the addition of 0.5% exopolysaccharide. Meanwhile, the paper clip observably corroded, accumulating black rust in the control solution. In the 0.5% HoEPS solution, however, only minor, localized corrosion, indicated by a thin black layer, occurred on the paper clip surface. This result indicates that the HoEPS from SK24.003 could prevent corrosion. In 0.5% amylopectin solution, there was some muddy precipitation in both calcium chloride and magnesium chloride solutions, which was due to the alignment of amylopectin chain (retrogradation) when the sample was stored at 30 °C for 7 days. Also, the

paper clip in salt solutions corroded with black rust as same as that in control solution. The difference in anticorrosion effect may be attributed to the structural features of glucan. Further studies need to be conducted to address this issue, which certainly would help us to understand the anticorrosive property in depth. As previously shown by Jones (1996), a magnesium chloride solution has a lower pH value than an equally concentrated calcium chloride solution. As illustrated in Fig. 6, there was less visible black material on the paper clip surface in the calcium chloride solution than in the magnesium chloride solution, which might be ascribed to the low pH of the magnesium chloride solution (pH 6.53). This could significantly alter the redox potential of Fe(II)/Fe(III). According to Finkenstadt et al. (2011), steel corrosion begins with the anodic oxidation of Fe to Fe(II). Fe(II) undergoes further oxidation to Fe(III), which then accelerates the conversion of Fe to Fe(II). The metal-HoEPS system, therefore, can inhibit corrosion by reducing the amount of electron acceptors at the interface by binding Fe(II) and Fe(III). A visual analysis of the corroding system indicated the formation of Fe(II) oxide (black) in the HoEPS system, whereas the flash corrosion present in the control system contained Fe(III) oxide (orange). The results suggested that the neutral HoEPS from the *L. reuteri* strain SK24.003 formed a barrier layer on the surface of steel and actively attenuated the corrosion process.

4. Conclusion

In this study, the neutral HoEPS-producing strain *L. reuteri* SK24.003 was isolated from a traditional Chinese fermented dairy product and identified. The exopolysaccharide was a typical homopolymeric glucan and has been indicated as a promising anti-corrosive for use in heavy-duty coatings. Its characterization suggested that the fine molecular structure might underlie its anticorrosive property. Further work is necessary to develop a more precise understanding of its mechanisms and structure–function relationship for potential industrial applications.

Acknowledgements

The research was financially supported by the National Natural Science Foundation of China (31000764, 31230057), National High Technology Research and Development Program of China (2013AA102102), International Cooperative Program of Jiangsu Province (BZ2012031) and Science & Technology Pillar Program of Jiangsu Province (BE2012613, BY2012049).

References

Ai, L., Zhang, H., Guo, B., Chen, W., Wu, Z., & Wu, Y. (2008). Preparation, partial characterization and bioactivity of exopolysaccharides from *Lactobacillus casei* LC2W. *Carbohydrate Polymers*, *74*, 353–357.

Badel, S., Bernardi, T., & Michaud, P. (2011). New perspectives for *Lactobacilli* exopolysaccharides. *Biotechnology Advances*, *29*, 54–66.

Bounaix, M. S., Gabriel, V., Morel, S., Robert, H., Rabier, P., Remaud-Simeon, M., et al. (2009). Biodiversity of exopolysaccharides produced from sucrose by sourdough lactic acid bacteria. *Journal of Agricultural and Food Chemistry*, *57*, 10889–10897.

Cakić, M., Mitić, Ž., Nikolić, G. S., Ilić, L., & Nikolić, G. M. (2008). The investigations of bioactive copper (II) complexes with reduced low-molar dextran. *Spectroscopy*, *22*, 177–185.

Cui, S. W. (2005). *Food carbohydrates: Chemistry, physical properties, and applications*. Boca Raton: CRC Press.

Dais, P., & Perlin, A. S. (1982). High-field, ^{13}C N.M.R. spectroscopy of β-D-glucans, amylopectin and glycogen. *Carbohydrate Research*, *100*, 103–116.

De Vuyst, L., De Vin, F., Vaningelgem, F., & Degeest, B. (2001). Recent developments in the biosynthesis and applications of heteropolysaccharides from lactic acid bacteria. *International Dairy Journal*, *11*, 687–707.

Finkenstadt, V. L., Côté, G. L., & Willett, J. L. (2011). Corrosion protection of low-carbon steel using exopolysaccharide coatings from *Leuconostoc mesenteroides*. *Biotechnology Letters*, *33*, 1093–1100.

Freitas, F., Alves, V. D., & Reis, M. A. M. (2011). Advances in bacterial exopolysaccharides: From production to biotechnological applications. *Trends in Biotechnology*, *29*, 388–398.

Gidley, M. J. (1985). Quantification of the structural features of starch polysaccharides by N.M.R. spectroscopy. *Carbohydrate Research*, *139*, 85–93.

Hassan, A. N. (2007). ADSA foundation scholar award: Possibilities and challenges of exopolysaccharide-producing lactic cultures in dairy foods. *Journal of Dairy Science*, *91*, 1282–1298.

Jones, D. A. (1996). *Principles and prevention of corrosion* (2nd ed.). UK: Prentice-Hall.

Kang, H. K., Kimura, A., & Kim, D. (2011). Bioengineering of *Leuconostoc mesenteroides* glucansucrases that gives selected bond formation for glucan synthesis and/or acceptor-product synthesis. *Journal of Agricultural and Food Chemistry*, *59*, 4148–4155.

Kumar, A. S., Mody, K., & Jha, B. (2007). Bacterial exopolysaccharides – A perception. *Journal of Basic Microbiology*, *47*, 103–117.

Leathers, T. D., & Côté, G. L. (2008). Biofilm formation by exopolysaccharide mutants of *Leuconostoc mesenteroides* strain NRRL B-1355. *Applied Microbiology and Biotechnology*, *78*, 1025–1031.

Leemhuis, H., Pijning, T., Dobruchowska, J. M., van Leeuwen, S. S., Kralj, S., Dijkstra, B. W., et al. (2013). Glucansucrases: Three-dimensional structures, reactions, mechanism, α-glucan analysis and their implications in biotechnology and food applications. *Journal of Biotechnology*, *163*, 250–272.

Maina, N. H., Tenkanen, M., Maaheimo, H., Juvonen, R., & Virkki, L. (2008). NMR spectroscopic analysis of exopolysaccharides produced by *Leuconostoc citreum* and *Weissella confusa*. *Carbohydrate Research*, *343*, 1446–1455.

Mitić, Ž., Cakić, M., & Nikolić, G. (2010). Fourier-Transform IR spectroscopic investigations of cobalt (II)–dextran complexes by using D_2O isotopic exchange. *Spectroscopy*, *24*, 269–275.

Mitić, Ž., Cakić, M., Nikolić, G. M., Nikolić, R., Nikolić, G. S., Pavlović, R., et al. (2011). Synthesis, physicochemical and spectroscopic characterization of copper(II)–polysaccharide pullulan complexes by UV–vis, ATR-FTIR, and EPR. *Carbohydrate Research*, *346*, 434–441.

Mitić, Ž., Nikolić, G. S., Cakić, M., Premović, P., & Ilić, L. (2009). FTIR spectroscopic characterization of Cu (II) coordination compounds with exopolysaccharide pullulan and its derivatives. *Journal of Molecular Structure*, *924–926*, 264–273.

Miao, M., Li, R., Jiang, B., Cui, S. W., Lu, K., & Zhang, T. (2014). Structure and digestibility of endosperm water-soluble α-glucans from different sugary maize mutants. *Food Chemistry*, *143*, 156–162.

Pan, D., & Mei, X. (2010). Antioxidant activity of an exopolysaccharide purified from *Lactococcus lactis* subsp. lactis 12. *Carbohydrate Polymers*, *80*, 908–914.

Penninga, N., Kralj, S., Euverink, G.-J., van der Maarel, M., van Geel-Schutten, I., & Dijkhuizen, L. (2002). GTF180: A glycosyltransferase producing a glucan with anti-corrosive properties. In *Proceedings of the Nederlandse Vereniging voor Medische Microbiologie* (p. 22).

Prajapati, V. D., Jani, G. K., Zala, B. S., & Khutliwala, T. A. (2013). An insight into the emerging exopolysaccharide gellan gum as a novel polymer. *Carbohydrate Polymers*, *93*, 670–678.

Roux, S., Bur, N., Ferrari, G., Tribollet, B., & Feugeas, F. (2010). Influence of a biopolymer admixture on corrosion behaviour of steel rebars in concrete. *Materials and Corrosion*, *61*, 1026–1033.

Santha, N., Sudha, K. G., Vijayakumari, K. P., Nayar, V. U., & Moorthy, S. N. (1990). Raman and infrared spectra of starch samples of sweet potato and cassava. *Journal of Chemical Sciences*, *102*, 705–712.

Scheerder, J., Breur, R., Slaghek, T., Holtman, W., Vennik, M., & Ferrari, G. (2012). Exopolysaccharides (EPS) as anti-corrosive additives for coatings. *Progress in Organic Coatings*, *75*, 224–230.

Seymour, F. R., Knapp, R. D., & Bishop, S. H. (1976). Determination of the structure of dextran by ^{13}C-nuclear magnetic resonance spectroscopy. *Carbohydrate Research*, *51*, 179–194.

Shingel, K. I. (2002). Determination of structural peculiarities of dexran, pullulan and γ-irradiated pullulan by Fourier-transform IR spectroscopy. *Carbohydrate Research*, *337*, 1445–1451.

Sreekumar, O., & Hosono, A. (1998). The antimutagenic properties of a polysaccharide produced by *Bifidobacterium longum* and its cultured milk against some heterocyclic amines. *Canadian Journal of Microbiology*, *44*, 1029–1036.

van Leeuwen, S. S., Leeflang, B. R., Gerwig, G. J., & Kamerling, J. P. (2008). Development of a ^{1}H NMR structural-reporter-group concept for the primary structural characterisation of α-D-glucans. *Carbohydrate Research*, *343*, 1114–1119.

Vinderola, G., Perdigón, G., Duarte, J., Farnworth, E., & Matar, C. (2006). Effects of the oral administration of the exopolysaccharide produced by *Lactobacillus kefiranofaciens* on the gut mucosal immunity. *Cytokine*, *36*, 254–260.